Measurement Science and Technology

PAPER

Eccentricity error identification and compensation for high-accuracy 3D optical measurement

Meas. Sci. Technol. **24** (2013) 075402 (7pp) doi:10.1088/0957-0233/24/7/075402

Eccentricity error identification and compensation for high-accuracy 3D optical measurement

Dong He[1], Xiaoli Liu[1], Xiang Peng[1,2], Yabin Ding[2] and Bruce Z Gao[3]

[1] Key Laboratory of Optoelectronic Devices and Systems of Ministry of Education and Guangdong Province, Shenzhen University, Shenzhen, Guangdong, 518060, People's Republic of China
[2] School of Mechanical Engineering, Tianjin University, Tianjin, 300072, People's Republic of China
[3] Department of Bioengineering, COMSET, Clemson University, Clemson, SC 29634, USA

E-mail: lxl@szu.edu.cn and xpeng@szu.edu.cn

Received 13 December 2012, in final form 8 May 2013
Published 17 June 2013
Online at stacks.iop.org/MST/24/075402

Abstract
The circular target has been widely used in various three-dimensional optical measurements, such as camera calibration, photogrammetry and structured light projection measurement system. The identification and compensation of the circular target systematic eccentricity error caused by perspective projection is an important issue for ensuring accurate measurement. This paper introduces a novel approach for identifying and correcting the eccentricity error with the help of a concentric circles target. Compared with previous eccentricity error correction methods, our approach does not require taking care of the geometric parameters of the measurement system regarding target and camera. Therefore, the proposed approach is very flexible in practical applications, and in particular, it is also applicable in the case of only one image with a single target available. The experimental results are presented to prove the efficiency and stability of the proposed approach for eccentricity error compensation.

Keywords: vision inspection, camera calibration, industrial optical metrology, spatial ellipse center, concentric circles, digital image processing

(Some figures may appear in colour only in the online journal)

1. Introduction

Three-dimensional (3D) optical measurements are involved in various techniques, such as camera calibration, vision metrology, close range photogrammetry and fringe projection profilometry (FPP) [1–5], where circular targets are widely used as signalizing control points. Because of the camera perspective projection, a circle is imaged as an ellipse and usually the center of the ellipse is not identical to the true projected center of the circular target, under this condition that the imaging plane and the circular target plane are not parallel to each other [6]. From the works of Ahn *et al* [7], the above deviation as eccentricity error is shown in figure 1 where the point C' is the center of circle, which is imaged on the point C. However the center of ellipse is at point B. The eccentricity error is just the deviation between C and B. The existence of eccentricity error will cause the inaccuracy of the 3D estimation.

Since circular targets are used as control points in many applications, it is quite an important task to identify and compensate the circular targets' eccentricity errors, especially for large-size targets in large-scale optical or vision metrology. In order to ensure high-accuracy measurement, several strategies have been proposed for identifying and compensating the eccentricity error. Zhang and Wei [6] built a position-distortion model and completed the numerical simulations of the eccentricity error. The major achievements are focused on the photogrammetry area. Aha *et al* [7] gave a complete mathematical description of the eccentricity error for a typical circular target imaged by camera considering the circle and target-imaging configuration parameters. More details will be discussed in section 2.

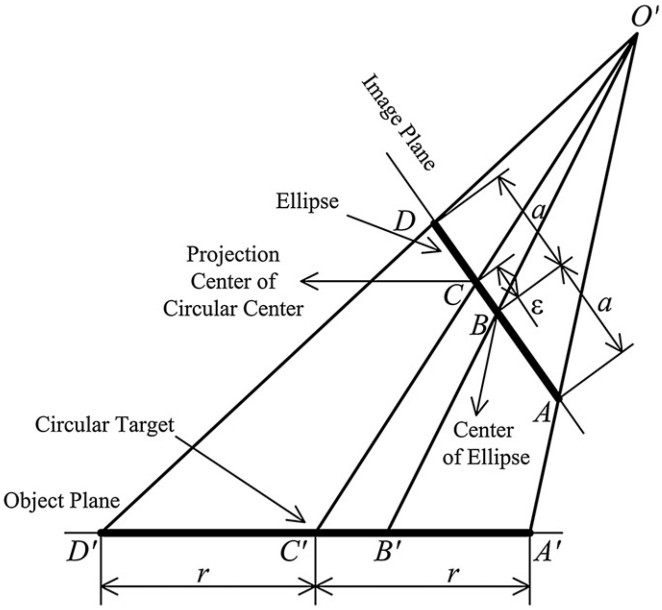

Figure 1. The principle of the eccentricity error.

Dold [8] studied how to estimate the suitable diameter of the circular target for high precision photogrammetric measurements, and also explored the impact of the eccentricity error on the 3D reconstruction with bundle adjustment (BA). In order to correct the eccentricity error with this mathematical model, one must accurately determine a number of parameters of the target-imaging configuration, and the parameters should be determined with the BA or camera calibration techniques. Recently, Otepka [9] and Otepka *et al* [10] predicted the rigorous relationship between a circular target and its perspective image through a new mathematical model; with the new model, the surface plane of circular targets can be automatically determined and the eccentricity error can be compensated. On the other hand, Heikkila and Silven [11] discussed the influence of eccentricity error on camera calibration, and constructed the error correction equations consisting of the geometric configuration parameters. However, the determination of these geometric parameters for correcting the eccentricity error is not easy. They solved this problem with the four-step camera calibration method.

Previous approaches mentioned above provide various mathematical descriptions about the eccentricity error of circular targets, and these mathematical models include the geometric parameters associated with the camera and circular targets. Thus an open issue to be addressed is how to determine these essential parameters in advance. Generally, this problem was solved by the techniques of camera calibration or BA strategy. However, in both cases, a number of circular targets in 3D space and their associated coordinates in 2D images are necessary to perform the calibration or BA, and the eccentricity errors are modeled by the additional parameters in the calibration or BA by adjustment based on least-squares methods (LSM), which involves one iterative process since the model is not linear. In this process, these additional parameters need to be estimated for correcting the eccentricity error. In consequence, it will increase the computation complexity and reduce convergence speed. To bypass this sensitive problem, we will introduce a novel method for identifying and compensating the eccentricity error of a circular target before the iterative process, where a concentric circles target (CCT) plays a key role. In previous studies, CCT is widely used in camera calibration and photogrammetry, and it normally has two usages: one as a control point [8–11], which is most common, and the other as a calibration object not a control point. In the second usage, the calibration arithmetic is based on the theorem of projective geometry [12–14], such as projective invariance, the unique properties of conic, the projective equation of a circle or CCT, etc. And in this paper, CCTs are used to compensate the eccentricity errors and, after this compensation, can be utilized to calibrate the camera. The mathematical description of the CCT eccentricity error is developed. Meanwhile, the corrected center will be determined by using a linear combination of two projected centers of ellipses formed by concentric circles. With this new method, the eccentricity errors can be identified and compensated without using any calibration parameters. In particular, this method is still valid in the case of only one available CCT and its associated image.

The rest of this paper is organized as follows: section 2 gives a brief review of the eccentricity error of a circular target reported by previous literature; section 3 introduces the CCT eccentricity error and develops a new compensation model for the eccentricity error of a circular target; section 4 presents the computer simulation and experiment results for compensating the eccentricity error; and section 5 summarizes the major points drawn from this study.

2. Eccentricity error of a circular target

Since Ahn *et al* [7] used a simple mathematical description to analyze the eccentricity error, we continue our study on this issue along their direction. As shown in figure 2, adapted from Ahn *et al* [7], three intermediate coordinate systems are introduced: the object coordinate system xyz with origin O, the camera coordinate system $x'y'z'$ with origin O' and the image coordinate system uv with origin H.

The coordinates of image point (u_c, v_c) (the image point of object target center C') in the image coordinate system Huv can be calculated as [7]

$$u_C = \frac{cx_p}{d\cos(\omega - \alpha)}$$
$$v_C = -c\tan(\omega - \alpha), \tag{1}$$

where c is the focal length of the camera lens; x_p is the x-coordinate of C' (center of circle) in the object coordinate system O_{xyx}; ω represents the angle between axis z and axis z' (the angle between the normal of circle and the optical axis of camera), that is the angle between the normal circular target and the normal camera imaging plane (same as the camera's optical axis direction); α represents the angle between axis z and the line OO' (the origin of the object coordinate system and the origin of the camera coordinate system); and d represents the exposure distance in the object coordinate system (the

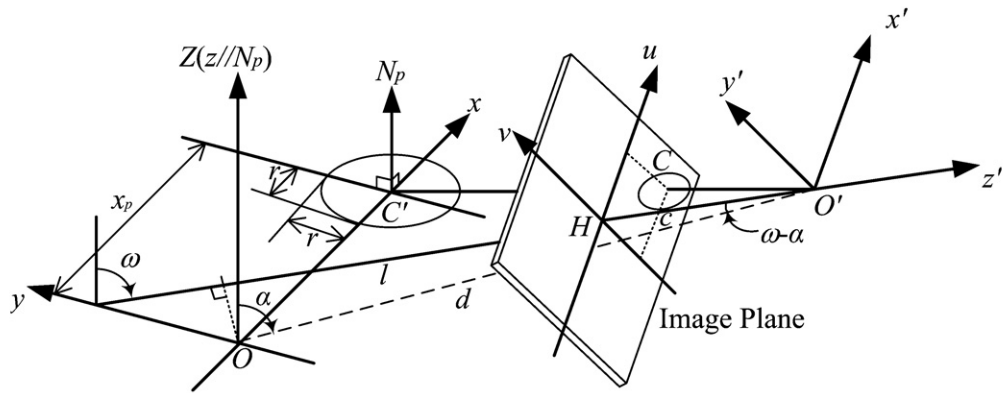

Figure 2. The camera model and intermediate coordinate systems.

distance between the origin O of the object coordinate system and the origin O' of the camera coordinate system).

The image point B (the center of the image ellipse) is represented by the following equation:

$$u_B = \frac{cx_p d\cos(\omega-\alpha)}{d^2\cos^2(\omega-\alpha) - r^2\sin^2\omega}$$
$$v_B = -c\frac{d^2\sin(\omega-\alpha)\cos(\omega-\alpha) + r^2\sin\omega\cos\omega}{d^2\cos^2(\omega-\alpha) - r^2\sin^2\omega}, \quad (2)$$

where d is the distance of OO', r is the radius of the circular target, and ω–α is the angle between the axis z' and the line OO'.

It can be seen (in figure 1) that the eccentricity errors in the image plane are characterized by the coordinate differences between two image points B and C. In the case of $l = d\cos(\omega-\alpha)$ (l is the distance of OO' projected on the optical axis direction), the eccentricity error can be obtained with equations (1) and (2):

$$\varepsilon_u = u_B - u_C = \frac{c(x_p/l)\sin^2\omega}{(l/r)^2 - \sin^2\omega}$$
$$\varepsilon_v = v_B - v_C = \frac{-c(d/l)\sin\omega\cos\omega}{(l/r)^2 - \sin^2\omega}. \quad (3)$$

For more details on how to deduce equations (1)–(3), the readers may refer to literature [7].

3. Eccentricity error of a CCT and new error-compensation model

From the eccentricity error equation (3), we can see that a number of geometric parameters such as ω, l, d, x_p and c must be determined before calculating the eccentricity error. However, it is difficult to obtain the accurate values of these geometric parameters without dedicated estimation techniques such as calibration or BA strategy. In order to avoid these troublesome calculations, we propose a new method to solve the problem of error-compensation. First, we recommend the usage of a CCT, which is shown in figure 3. In the perspective projection, the shapes of two circles are changed to two different ellipses. In figure 3, C is the center of the CCT, B_1 and B_2 are the centers of the ellipses, respectively. It is observed that the eccentricity errors of the two circles do not coincide with each other due to the deviation of their radii (also seen in equation (3)).

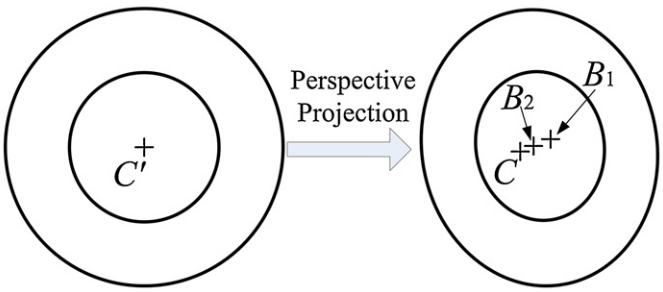

Figure 3. The shape of the CCT and its deformed image with perspective projection.

In the actual camera imaging model, $l \gg r$ and $\sin^2\omega < 1$, so $(l/r)^2 \gg \sin^2\omega$. Therefore, we can neglect the term $\sin^2\omega$ in the denominator of (3). Then equation (3) becomes

$$\varepsilon_u = u_B - u_C \approx \frac{c(x_p/l)\sin^2\omega}{(l/r)^2} = K_u \cdot r^2$$
$$\varepsilon_v = v_B - v_C \approx \frac{-c(d/l)\sin\omega\cos\omega}{(l/r)^2} = K_v \cdot r^2, \quad (4)$$

where $K_u = cx_p\sin^2\omega/l^3$ and $K_v = -cd\sin\omega\cos\omega/l^3$ are two coefficients that are not functions of the radius r. Therefore, for two circles of a CCT, their coefficients K_u, K_v are respectively equal, except for the radius r.

With two concentric circles of the CCT, two equations can be developed as follows:

$$\begin{cases} \varepsilon_{u1} = u_{B_1} - u_C = K_u \cdot r_1^2 \\ \varepsilon_{v1} = v_{B_1} - v_C = K_v \cdot r_1^2 \end{cases} \quad (5)$$

$$\begin{cases} \varepsilon_{u2} = u_{B_2} - u_C = K_u \cdot r_2^2 \\ \varepsilon_{v2} = v_{B_2} - v_C = K_v \cdot r_2^2 \end{cases}. \quad (6)$$

In the above equations, r_1, r_2 are the radii of larger and smaller circles, (u_{B_1}, v_{B_1}), (u_{B_2}, v_{B_2}) are the centers of larger and smaller ellipses, correspondingly. In order to solve the center (u_C, v_C) of the CCT, equations (5) and (6) should be combined to establish a closed-form solution described as follows:

$$u_C = k_1 u_{B_2} - k_2 u_{B_1}$$
$$v_C = k_1 v_{B_2} - k_2 v_{B_1}, \quad (7)$$

where $k_1 = r_1^2/(r_1^2 - r_2^2)$, $k_2 = r_2^2/(r_1^2 - r_2^2)$. The factors k_1, k_2 can be simply calculated with the known radii r_1, r_2. The centers of two ellipses (u_{B_1}, v_{B_1}), (u_{B_2}, v_{B_2}) can be detected by some image processing techniques. Now the eccentricity error is compensated by using the set of linear equation (7).

The above discussion is under the ideal lens without distortion; however, distortion is unavoidable [15]; and in many camera calibration methods [16–20] the lens distortions are seen as additional parameters, including the radial, de-centering and affine distortion [20]. In order to prove that the proposed compensation model is still valid while considering the lens distortions, further explanations are as follows: after adding lens distortions, the centers of ellipse are $B\prime_1(u_{B_1}+\Delta u_1, v_{B_1}+\Delta v_1)$, $B\prime_2(u_{B_2}+\Delta u_2, v_{B_2}+\Delta v_2)$, where Δu_1, Δv_1, Δu_2, Δv_2,are the lens distortions containing all its components, regardless of the model used. Since the centers of the bigger and smaller ellipses B_1, B_2 are very close, the distortions at locations B_1 and B_2 are nearly the same. We can assume that $\Delta u_1 = \Delta u_2 = \Delta u$, $\Delta v_1 = \Delta v_2 = \Delta v$. Under this assumption, equation (7) can be written as

$$\begin{aligned} u'_c &= k_1\left(u_{B_2}+\Delta u\right) - k_2\left(u_{B_1}+\Delta u\right) = k_1 u'_{B_2} - k_2 u'_{B_1} \\ v'_c &= k_1\left(v_{B_2}+\Delta v\right) - k_2\left(v_{B_1}+\Delta v\right) = k_1 v'_{B_2} - k_2 v'_{B_1}. \end{aligned} \tag{8}$$

In equations (8), $B'_1\left(u'_{B_1}, v'_{B_1}\right)$, $B'_2(u'_{B2}, v'_{B2})$ are the centers of the two ellipses, which are detected by digital image processing; and $C'_2(u'_c, v'_c)$ is the center of the CCT after compensating the eccentricity but containing the lens distortion. By the above analysis, we can draw a conclusion that the coordinate of the CCT center C is the linear combination of the coordinates of the two ellipses' centers B_1, B_2 including lens distortion. It should be noted that the eccentricity error can also be represented by the linear combination of the coordinates of the two ellipse centers by contrasting equations (7) and (8). By comparing equations (1) or (3) with equation (7), we can see that the geometric parameters are no longer required. Instead, we need to locate two centers of ellipses, which is simpler than estimating geometric parameters by using a calibration process or BA strategy as done in previous approaches.

4. Simulation and experimental results

To demonstrate the validity of the proposed method, a few experiments were conducted on both computer simulation and real experiment.

4.1. Computer simulation

The simulated camera has the following specifications: the resolution is 1280 × 1024 pixels, the principal point (pp) coordinates are expressed in pixels, as the following: $u_0 = 640$ pixels, $v_0 = 512$ pixels, the focal length is $c = 12$ mm. The ratio of radii r_1/r_2 is fixed as 2 ($r_1 = 2r_2$). In this case, the coefficients are $k_1 = 4/3$, $k_2 = 1/3$. The sub-pixel centers of the two ellipses (u_{B_1}, v_{B_1}), (u_{B_2}, v_{B_2}) were detected with the ellipse center location approach [21, 22]. Then the CCT corrected center was determined with equation (7). The corrected center was then compared with the ground truth, and the eccentricity error can be estimated as the Euclidean distance between the corrected center point and true center point measured in pixels.

Table 1. The values of eccentricity errors (EEs) with respect to the radius of the larger circle.

Radius (mm)	EEs (pixels)
5	4.8×10^{-7}
10	5.4×10^{-6}
15	2.4×10^{-5}
20	7.2×10^{-5}
25	1.7×10^{-4}
30	3.4×10^{-4}
35	6.2×10^{-4}
40	1.0×10^{-3}
45	1.7×10^{-3}
50	2.5×10^{-3}
55	3.6×10^{-3}
60	5.1×10^{-3}

Table 2. The values of eccentricity errors (EEs) with respect to the angle ω.

Angle (radians)	EEs (pixels)
$\pi/15$	4.3×10^{-6}
$2\pi/15$	2.9×10^{-5}
$3\pi/15$	8.0×10^{-5}
$4\pi/15$	1.2×10^{-4}
$5\pi/15$	1.6×10^{-4}
$6\pi/15$	1.3×10^{-4}
$7\pi/15$	7.7×10^{-5}

4.1.1. Performance with respect to the radius of CCT. In order to simplify the calculation, the structure parameters are assumed as $\omega = \pi/4$, $d = 800$ mm and $\alpha = \omega$, then $l = d = 800$ mm. The radius r_1 is set from 0 to 60 mm with 5 mm intervals, and the ratio remains constant ($r_1/r_2 = 2$). Figure 4(*a*) shows the eccentricity errors by using our method, where '□' represents the distance (eccentricity error) between the estimated center using our approach and the true center of the CCT; and figure 4(*b*) shows the result using the ellipse fitting method, where '○' represents the distance (eccentricity error) between the center of the fitted ellipse and the true center of the CCT. It can be seen that the ellipse centers gradually deviate from the true center of the CCT as the radius value increases; obviously it cannot identify the eccentricity error. It can be seen that our approach can efficiently compensate the eccentricity error, even when the radius value is very large. In order to see more clearly, table 1 shows the concrete values of the eccentricity error. The eccentricity error is enlarged with increase of the radius of the CCT. However, the maximum error does not exceed the accuracy of sub-pixel levels with the center location method [21, 22] (0.01 pixels).

4.1.2. Performance with respect to the angle ω. This experiment investigates the performance with respect to angle ω. In the experiment, the radii of the smaller and larger circles are set to 12 and 24 mm, respectively, and the angle ω is assumed to be from $\pi/15$ to $7\pi/15$ with an interval of $\pi/15$. The simulation result is as follows: the eccentricity errors obtained by our method are shown in figure 5(*a*), and the results obtained by the ellipse-fitting method are shown in figure 5(*b*). Table 2 shows that the concrete values of the error

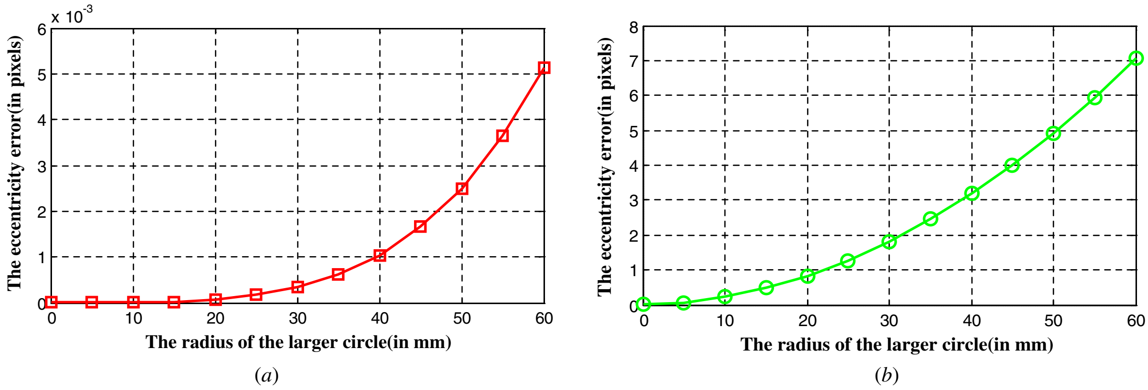

Figure 4. (*a*) The eccentricity errors of center location with respect to the radius with our method, (*b*) with the ellipse fitting method.

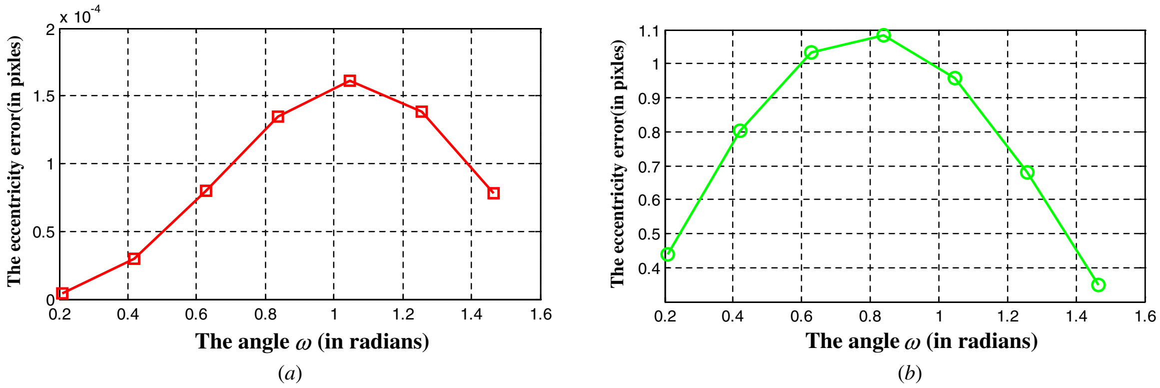

Figure 5. (*a*) The eccentricity errors of center location with respect to the angle ω with our method, (*b*) with the ellipse fitting method.

are very small after correction by our method. The errors are changed with the variation of angle ω by using the ellipse-fitting method; and with our approach, the eccentricity error can be kept at a very low level.

4.2. Experiment by using real data

In the experiment, we printed a CCT, where the radii of the larger and smaller circles were 120 and 60 mm, and the CCT center was marked with '+' on the pattern. A Daheng CMOS camera with a resolution of 1280 × 1024 pixels was used to capture the image of the CCT. The exposure distance between the camera and CCT was about 1.0 m, and the angle between the normal CCT and the optical imaging axis was about 45°. Figure 6 shows the center identification results using equation (7). The red '+' represents the location of the center of the smaller circle obtained by image processing techniques [21, 22]; the red '∗' represents the location of the center of the larger circle; and the blue '+' is the location of the CCT center identified by our method. Experiment results showed good accordance with the true CCT center predicted by the theoretical model. It should be especially pointed out that this experiment was performed successfully without considering the estimate of any calibration parameters (include exterior and inner orientation parameters) but using only one image of a single CCT. Moreover, the eccentricity error has also been greatly compensated by locating the center of the CCT with our method.

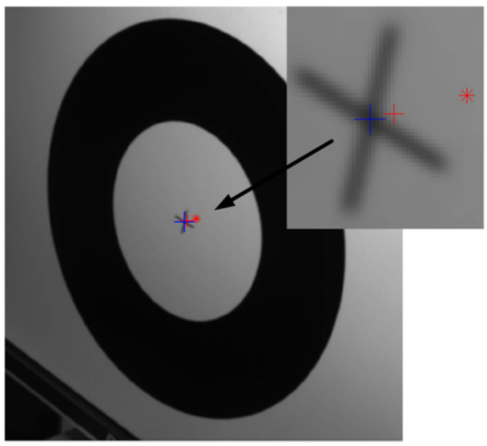

Figure 6. Correction results for one image of a single CCT.

In order to compare the method presented by Ahn *et al* [7] (referred to hereafter as 'the compared method') with ours, we need to calculate the calibration parameters in advance. Therefore, a standard plane with 58 CCTs was used for camera calibration, and these CCT-coordinates in the 3D space had been determined, as shown in figure 7. The radius of the smaller circle was 2.5 mm and the radius of the larger circle was 5.0 mm. In our method, both circles of the CCTs were used, but only smaller CCTs were employed in the compared method. In addition, there were five coded markers, which were used to automatically search for the corresponding CCTs among

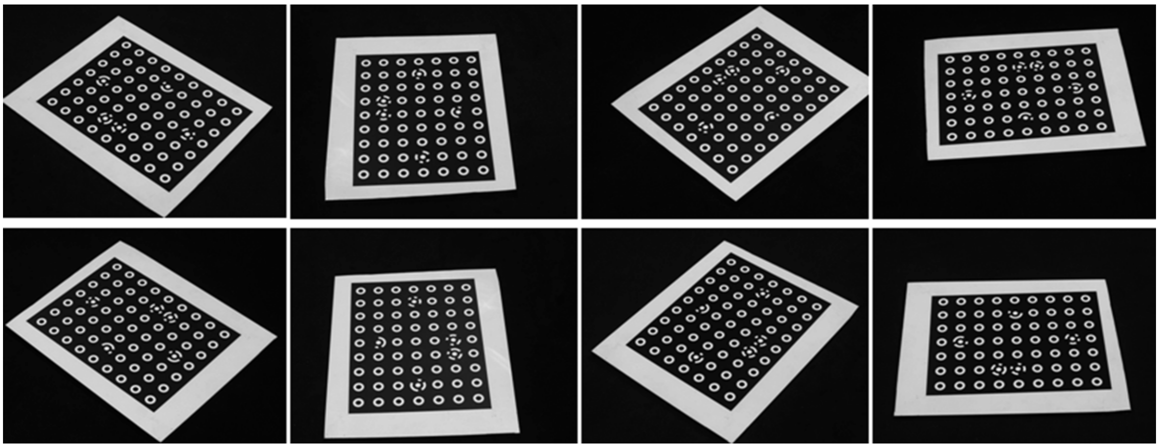

Figure 7. The eight images of the plane with 58 CCTs taken from eight different viewpoints.

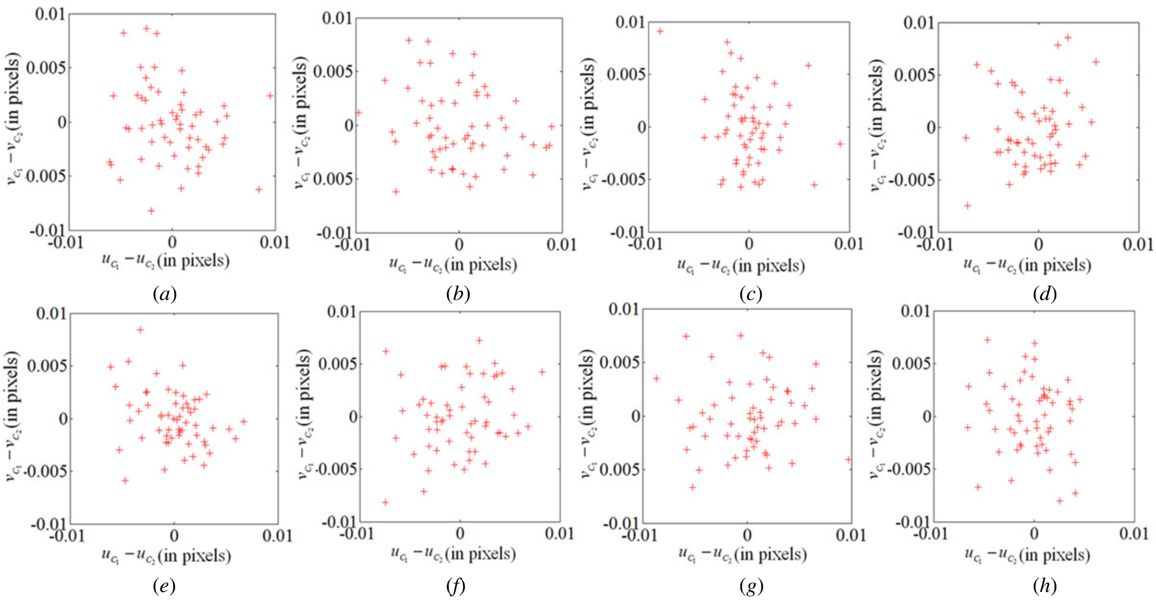

Figure 8. The deviations of identified centers between the compared method and ours; plots (*a*)–(*h*) represent eight different images.

the images. In order to determine the calibration parameters for the compared method, the ImagingSource CCD camera with resolution of 1280 × 960 pixels was used to capture eight images of the CCTs from eight different viewpoints. Then we detected and located the coordinates of the centers of smaller ellipses (the circle of the CCT changes to an ellipse under the perspective projection) in eight images. With the coordinates of ellipse centers in 3D space and in images, the required parameters were estimated by Zhang's calibration method [23]. The calibration parameters were employed to correct the center of the centers of CCTs $C_1(u_{C_1}, v_{C_1})$ with equation (3), in the compared method. On the other hand, we identified the center of the CCTs $C_2(u_{C_2}, v_{C_2})$ with our method only using equation (7). In our approach, both the centers of larger and smaller ellipses were determined simultaneously, which led to the elimination of the troublesome process of the necessary parameters' estimation for compensating the eccentricity errors. In order to compare the differences of identified centers' coordinates between the two methods, we calculated the deviation between $C_1(u_{C_1}, v_{C_1})$ and $C_2(u_{C_2}, v_{C_2})$, and illustrated the differences $C_1 - C_2(u_{C_1} - u_{C_2}, v_{C_1} - v_{C_2})$ for eight images; in figure 8, 58 '+' implied that there were 58 CCTs in each image. The values of $u_{C_1} - u_{C_2}$ and $v_{C_1} - v_{C_2}$ were illustrated in horizontal and vertical axes, respectively. The unit was measured in pixels. It could be seen that the deviations are smaller than 0.01 pixels under the influence of imaging noise. In common, the location error was less than 0.02 pixels in the center location techniques. Therefore, it would not affect the accuracy of measurement. Note that our method can achieve the same accuracy level as that with the compared method. However, our method does not need to determine those parameters associated with the CCTs and the camera. It is more flexible for various measurement applications.

5. Conclusion

In conclusion, we have proposed a new approach for correcting the eccentricity error of a circular target with the use of a pattern of two concentric circles instead of a single circle pattern. Linear center-identification equations are developed by using an approximate description regarding eccentricity error. Compared with those approaches previously reported, the new correction approach eliminates the need of calibration parameters that are usually used to estimate the eccentricity errors. Both computer simulation and practical experiment have been performed, which have demonstrated the efficiency and stability of the proposed method. As a systematic error, the eccentricity error can be successfully compensated. Because the camera parameters are no longer required, the proposed correction method can also be used in high-accuracy 3D measurement in a simple way, such as camera calibration, close range photogrammetry, vision measurement and FPP calibration.

Acknowledgments

The authors would like to acknowledge the financial support from the Natural Science Foundation of China under grant nos 61171073, 61003178, the Sino-German Center for Research Promotion under grant GZ 760 (Remote Laboratory for Optical Micro Metrology), the Scientific and Technological Project of the Shenzhen government. Two joint research projects sponsored by Tianjin University and Shenzhen University, and the State Key Laboratory of Virtual Reality Technique and System are also gratefully acknowledged.

References

[1] Peng X, Liu X, Yin Y and Li A 2011 Optical measurement network for large-scale and shell-like objects *Opt. Lett.* **36** 157–9

[2] Zhang S and Huang P S 2006 Novel method for structured light system calibration *Opt. Eng.* **45** 083601

[3] Atkinson K B 2003 *Close Range Photogrammetry and Machine Vision* (Caithness: Whittles Publishing)

[4] Zhang Z, Ma H, Zhang S, Guo T, Towers E C and Towers D P 2011 Simple calibration of a phase-based 3D imaging system based on uneven fringe projection *Opt. Lett.* **36** 627–9

[5] Gai S and Da F 2010 Fringe image analysis based on the amplitude modulation method *Opt. Express* **18** 10704–19

[6] Zhang G and Wei Z 2003 A position-distortion model of ellipse centre for perspective projection *Meas. Sci. Technol.* **14** 1420–6

[7] Ahn S J, Warnecke H J and Kotowski R 1999 Systematic geometric image measurement errors of circular object targets: mathematical formulation and correction *Photogramm. Rec.* **16** 485–502

[8] Dold J 1996 Influence of large targets on the results of photogrammetric bundle adjustment *Int. Arch. Photogramm. Remote Sens.* **31** 119–23

[9] Otepka J 2004 Precision target mensuration in vision metrology *PhD Thesis* Vienna University of Technology, Austria

[10] Otepka J and Fraser C S 2005 Measurement eccentricities of circular targets in vision metrology *Proc. Optical 3-D Measurement Techniques Congress*

[11] Heikkilä J and Silvén O 1997 A four-step camera calibration procedure with implicit image correction *IEEE Computer Society Conf. on Computer Vision and Pattern Recognition* pp 1106–12

[12] Zhao Z and Liu Y 2010 Applications of projected circle centers in camera calibration *Mach. Vis. Appl.* **21** 301–7

[13] Ma W, Zheng Y and Liu Y 2009 Camera calibration using two concentric circles: linear approach *Opt. Eng.* **48** 053602

[14] Morde A, Bouzit M and Rabiner L 2006 A novel approach to planar camera calibration *Int. Conf. on Computer Vision Theory and Applications* pp 87–92

[15] Brown D C 1971 Close-range camera calibration *Photogramm. Eng.* **37** 855–66

[16] Clarke T A and Fryer J G 1998 The development of camera calibration methods and models *Photogramm. Rec.* **16** 51–66

[17] Chandler J H, Fryer J G and Jack A 2005 Metric capabilities of low-cost digital cameras for close range surface measurement *Photogramm. Rec.* **20** 12–26

[18] Fryer J G and Brown D 1986 Lens distortion for close-range photogrammetry *Photogramm. Eng. Remote Sens.* **52** 51–8

[19] Fraser C S 1997 Digital camera self-calibration ISPRS *J. Photogramm. Remote Sens.* **52** 149–59

[20] Habib A and Morgan M 2005 Stability analysis and geometric calibration of off-the-shelf digital cameras *Photogramm. Eng. Remote Sens.* **71** 733–41

[21] Fitzgibbon A, Pilu M and Fisher R B 1999 Direct least squares fitting of ellipses *IEEE Trans. Pattern Anal. Mach. Intell.* **21** 476–80

[22] Da F and Zhang H 2010 Sub-pixel edge detection based on an improved moment *Image Vis. Comput.* **28** 1645–58

[23] Zhang Z 2000 A flexible new technique for camera calibration *IEEE Trans. Pattern Anal. Mach. Intell.* **22** 1330–4